CANCELLING SELF-INTERFERENCE IN FULL-DUPLEX RELAYS WITHOUT ANGLE-OF-ARRIVAL INFORMATION

Emilio Antonio-Rodríguez[*]

Galician R&D Center in
Advanced Telecommunications (GRADIANT)
Vigo, Spain

Roberto López-Valcarce[*]

Dept. Signal Theory & Communications
University of Vigo
Vigo, Spain

ABSTRACT

With full-duplex relays, simultaneous reception and transmission in the same frequency produce self-interference distortion and relay oscillation, hampering reception at the receiver end unless properly mitigated. Previous adaptive methods for self-interference cancellation using multiple receive antennas require knowledge of the direction of arrival of the source signal. We present a novel architecture and adaptive scheme for Amplify-and-Forward relays allowing cancellation without such knowledge. The temporal filter is updated under the property restoral paradigm in order to match the power spectrum of the retransmitted signal to that of the source signal.

Index Terms— Full-duplex relays, adaptive filters, feedback cancellation, MISO, spectrum shaping, beamforming.

1. INTRODUCTION

Self-interference at relays is a direct consequence of simultaneous transmission and reception (full-duplex mode [1, 2]) in the same frequency, which creates a feedback path between the transmit and receive side of the relay [3]. Even if some degree of antenna isolation is provided by design, this may be insufficient, given that the retransmitted signal power is usually tens of dB above that of the received signal from the source. If not properly dealt with at the relay, this self-interference will hamper demodulation at the final destination. Consequently, full-duplex relays must include self-interference mitigation techniques [4, 5, 6, 7]. We presented in [8] a novel adaptive suppressor for Amplify-and-Forward (A&F) relays [9] equipped with a single receive and a single transmit antenna (SISO). This adaptive filter, whose operating principle is the restoral of the desired power spectrum at the relay output, has low complexity and provides good performance without introducing additional processing delay in the relay station (which is undesired for cyclic prefix-based modulation formats). This design was extended in [10] to relays with multiple receive antennas (MISO), effectively combining temporal processing (filtering) and spatial processing (beamforming) in order to provide further supression of the unwanted feedback signal. However, one drawback of the design from [10] is the need to know the angle of arrival (AoA) of the incoming source signal for the adaptation of the beamformer, thus reducing its leeway. We aim to overcome this issue by extending the methods from [8] and [10] to a fully integrated spatio-temporal adaptive feedback suppressor which does not require AoA knowledge for its operation.

[*]Supported by the European Regional Development Fund (ERDF) and the Spanish Government under projects DYNACS (TEC2010-21245-C02-02/TCM) and COMONSENS (CONSOLIDER-INGENIO 2010 CSD2008-00010), and the Galician Regional Government under projects ESCOLMA (10TIC013CT) and "Consolidation of Research Units: AtlantTIC" (CN 2012/260).

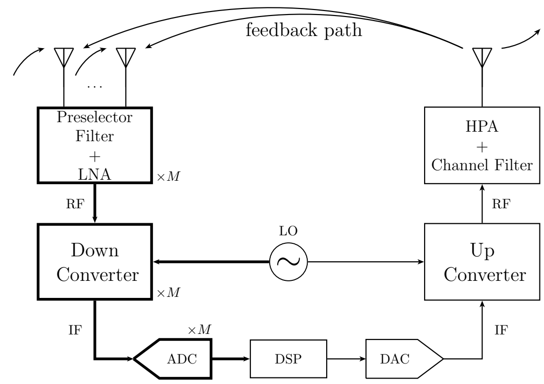

Fig. 1. MISO M-input, 1-output wireless relay.

2. PROBLEM FORMULATION

The block diagram of a MISO A&F full-duplex relay is shown in Fig. 1, consisting of: (i) The M receive analog front-ends, each comprising a receive antenna and a down-conversion stage either to baseband or to an intermediate frequency (IF); (ii) The digital stage, consisting of the M analog-to-digital converters (ADC), a digital signal processing (DSP) unit implementing the space-time feedback suppressor (STFS), and the corresponding digital-to-analog converter (DAC); (iii) The transmit analog front-end, comprising the up-conversion stage to RF, a high-power amplifier, a channel filter to reduce out-of-band emissions and the transmit antenna.

A discrete-time equivalent model is presented next. The underlying sampling rate is $f_s = 1/T_s$. The incoming signal from the source (assumed to be a single-antenna transmitter), with bandwidth much smaller than the carrier frequency, is denoted by $s(n)$. The source-relay channel, assumed time-invariant[1], is modeled as a multipath channel with N_s propagation paths [11]:

$$\boldsymbol{d}(\omega) = \sum_{i=0}^{N_s-1} \beta_i^{(s)} \boldsymbol{v}(\phi_i^{(s)}) e^{-j\omega\Delta_i^{(s)}/T_s}, \tag{1}$$

where $\beta_i^{(s)}$, $\Delta_i^{(s)}$ and $\phi_i^{(s)}$ are respectively the gain, delay and AoA

[1]The adaptive schemes presented in the sequel should be able to track time variations as long as these are sufficiently slow.

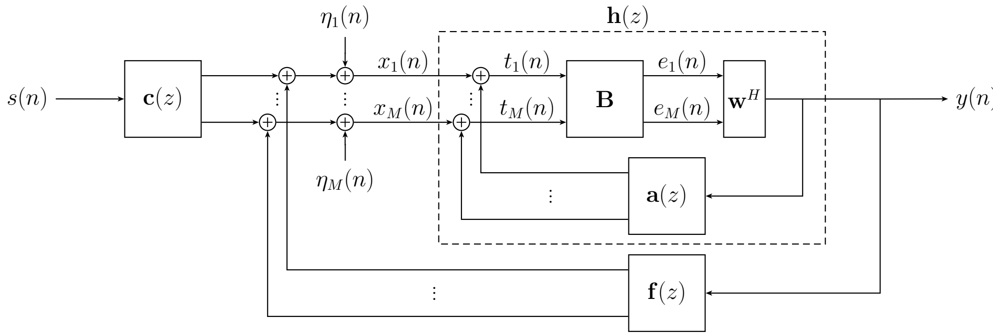

Fig. 2. Equivalent baseband representation of the MISO A&F relay. The dashed box contains the feedback supressor.

of the i-th path. The array response [12] is denoted by $\boldsymbol{v}(\phi)$. For example, for a uniform linear array (ULA) as considered in Sec. 5 one has $\boldsymbol{v}(\phi) = [\ 1 \quad e^{j\theta} \quad \cdots \quad e^{j(M-1)\theta}\ ]^H$, with $\theta = \frac{2\pi d}{\lambda}\sin\phi$, and λ, d respectively the carrier wavelength and element separation.

Analogously to (1), the coupling channel between the relay transmit antenna and its receive array is modeled as

$$\boldsymbol{p}(\omega) = \sum_{i=1}^{N_r} \beta_i^{(r)} \boldsymbol{v}(\phi_i^{(r)}) e^{-j\omega\Delta_i^{(r)}/T_s}. \qquad (2)$$

We will denote by $\boldsymbol{d}(z) = \sum_{i=0}^{L_d} \boldsymbol{d}_i z^{-i}$ and $\boldsymbol{p}(z) = \sum_{i=1}^{L_p} \boldsymbol{p}_i z^{-i}$ the z-domain versions of (1) and (2) respectively. Similarly, the z-domain equivalent of the j-th analog front-end at the receive side is denoted by $g_j(z)$, $1 \le j \le M$, whereas that of the analog front-end at the transmit side is denoted by $g_0(z)$.

Fig. 2 shows the baseband equivalent system of the relay from the STFS perspective, where we have introduced the equivalent source-to-relay and coupling transfer functions $\boldsymbol{c}(z) \doteq \boldsymbol{G}(z)\boldsymbol{d}(z)$ and $\boldsymbol{f}(z) \doteq \boldsymbol{G}(z)\boldsymbol{p}(z)g_0(z)$, respectively, with $\boldsymbol{G}(z) \doteq \text{diag}\{g_1(z) \ \cdots \ g_M(z)\}$. We then write

$$\boldsymbol{c}(z) = \sum_{i=0}^{L_c} \boldsymbol{c}_i z^{-i}, \quad \boldsymbol{f}(z) = \sum_{i=1}^{L_f} \boldsymbol{f}_i z^{-i}. \qquad (3)$$

Note that $\boldsymbol{f}(z)$ is strictly causal. It is also assumed that $\boldsymbol{c}_0 \neq \mathbf{0}$, since the proposed algorithm is based on second-order statistics of $s(n)$ and hence remains insensitive to a bulk delay factor in $\boldsymbol{c}(z)$.

The vector $\boldsymbol{\eta}(n) = [\eta_1(n) \ \ldots \ \eta_M(n)]^T$ denotes the input noise, whereas $y(n)$ is the retransmitted signal. The M-input, 1-output STFS transfer function $\boldsymbol{h}(z)$ is comprised of three blocks: an $M \times M$ diagonal matrix $\boldsymbol{B} = \text{diag}\{b_1 \ \cdots \ b_M\}$ with complex-valued gains b_i; an $M \times 1$ vector $\boldsymbol{w} = [w_1 \cdots w_M]^T$; and a 1-input, M-output filter with (strictly causal) transfer function $\boldsymbol{a}(z) = \sum_{i=1}^{L_a} \boldsymbol{a}_i z^{-i}$. With these, the relay output $y(n)$ becomes

$$y(n) = \frac{\boldsymbol{w}^H \boldsymbol{B}}{1 - \boldsymbol{w}^H \boldsymbol{B}\left[\boldsymbol{f}(z) + \boldsymbol{a}(z)\right]} \left[\boldsymbol{c}(z)s(n) + \boldsymbol{\eta}(n)\right] \qquad (4)$$

Eq. (4) shows the effect of the coupling path, which can be seen as an IIR channel at the destination. With the architecture proposed, an obvious choice to eliminate this effect is to select $\boldsymbol{w}^H \boldsymbol{B}\boldsymbol{a}(z) = -\boldsymbol{w}^H \boldsymbol{B}\boldsymbol{f}(z)$. The challenge is to design suitable adaptive schemes in order to achieve this solution blindly, i.e. without knowledge of the coupling transfer function $\boldsymbol{f}(z)$ or the source-relay channel $\boldsymbol{c}(z)$.

The STFS architecture in Fig. 2 cancels the feedback *before* combining the M incoming signals. This is in contrast with the approach in [10], in which spatial combining (beamforming) is done first, and then feedback cancellation is applied. As we will see, this modification allows for the derivation of adaptive schemes which do not require AoA knowledge. On the other hand, the architecture in Fig. 2 makes use of M temporal filters (the entries of $\boldsymbol{a}(z)$), whereas the scheme from [10] requires a single temporal filter.

3. ADAPTIVE ALGORITHM

In the proposed architecture (Fig. 2), the effective beamformer is $\boldsymbol{u} \doteq \boldsymbol{B}^H \boldsymbol{w}$, and at first sight, splitting $\boldsymbol{u}$ into two components $\boldsymbol{B}$ and $\boldsymbol{w}$ may seem redundant. The reason for this parameterization has to do with the particularities of the adaptive algorithm. The adaptive parameters of the STFS are $\boldsymbol{B}$ (for spatial processing) and $\boldsymbol{a}(z)$ (for temporal processing), whereas $\boldsymbol{w}$ is fixed. The choice of $\boldsymbol{w}$ is related to any *a priori* knowledge regarding the SNR distribution among the M antennas; lacking such knowledge, one may just fix $\boldsymbol{w} = \mathbf{1}$ (the all-ones vector).

The update rule is inspired by [8] which, for the single-antenna case, forces the autocorrelation of the output signal $y(n)$ to match that of the source signal $s(n)$. With $M > 1$ antennas, such approach is not directly applicable since the number of parameters exceeds the number of autocorrelation-matching constraints. To circumvent this problem, we propose instead to have the cross-correlation of each of the signals $e_i(n)$, $i = 1, \ldots, M$ (the outputs of the adaptive spatial processor $\boldsymbol{B}$, see Fig. 2) and the output signal $y(n)$ match the autocorrelation of $s(n)$, appropriately scaled by the corresponding entry of the fixed vector $\boldsymbol{w}$. Specifically, let

$$\boldsymbol{e}(n) \doteq [\ e_1(n) \quad \cdots \quad e_M(n)\ ]^T, \qquad (5)$$

$$r_k \doteq \mathbb{E}\{s(n)s^*(n-k)\}. \qquad (6)$$

Similarly to [8, 10], it is assumed that the relay has knowledge of the autocorrelation $\{r_k\}$, which is very reasonable in practice. Now letting $\boldsymbol{b} \doteq [b_1 \ \cdots \ b_M]^T$ comprise the elements in the diagonal of $\boldsymbol{B}$, the update equations are as follows:

$$\boldsymbol{b}(n+1) = \boldsymbol{b}(n) + \mu_b \boldsymbol{B}(n)\left[r_0 \boldsymbol{w} - \boldsymbol{e}(n)y^*(n)\right], \qquad (7)$$

$$\boldsymbol{a}_k(n+1) = \boldsymbol{a}_k(n) + \mu_a \boldsymbol{B}^{-1}(n) \times \left[r_k \boldsymbol{w} - \boldsymbol{e}(n)y^*(n-k)\right], \ k = 1, \ldots, L_a, \qquad (8)$$

with μ_a, μ_b positive stepsizes. Note that in contrast with [10] this algorithm does not require any side information about the spatial properties (e.g. AoA) of the incoming signal. The adaptive scheme (7)-(8) boils down to that in [8] when $M = 1$, except for the presence of the diagonal factors $\boldsymbol{B}(n)$, $\boldsymbol{B}^{-1}(n)$ in the respective update terms. The inclusion of these factors is due to stability considerations; if left out, ill-convergence may occur, as we have observed in many simulation runs. Whereas a stability analysis of (7)-(8) will be presented elsewhere, next we focus on the characterization of the stationary points.

4. ANALYSIS

4.1. Stationary point conditions

At any stationary point of (7)-(8), the expected value of the update terms must vanish, i.e.

$$\mathbb{E}\{\boldsymbol{e}(n)y^*(n-k)\} = r_k \boldsymbol{w}, \quad k = 0, 1, \ldots, L_a. \tag{9}$$

Let $\mathsf{S}_{uv}(z)$ denote the power cross-spectrum of the processes $u(n)$, $v(n)$. If the number of coefficients L_a of the adaptive (temporal) filter is sufficiently large, then (9) implies that the causal parts of $\mathsf{S}_{\boldsymbol{e}y}(z)$ and $\mathsf{S}_{ss}(z)\boldsymbol{w}$ must be equal. Since these cross-spectra have Hermitian symmetry (note that $\mathsf{S}_{\boldsymbol{e}y}(z) = \mathbf{S}_{\boldsymbol{ee}}(z)\boldsymbol{w}$), this yields

$$\mathbf{S}_{\boldsymbol{ee}}(z)\boldsymbol{w} = \mathsf{S}_{ss}(z)\boldsymbol{w}, \qquad \text{for sufficiently large } L_a, \tag{10}$$

revealing that at any stationary point $(\mathsf{S}_{ss}(z), \boldsymbol{w})$ is an eigenpair of $\mathbf{S}_{ee}(z)$. Since $y(n) = \boldsymbol{w}^H \boldsymbol{e}(n)$, from (10) one has

$$\mathsf{S}_{yy}(z) = \boldsymbol{w}^H \mathbf{S}_{\boldsymbol{ee}}(z)\boldsymbol{w} = |\gamma|^2 \mathsf{S}_{ss}(z), \tag{11}$$

where $|\gamma|^2 \doteq ||\boldsymbol{w}||^2$. Therefore, at any stationary point the power spectrum of the relay output $y(n)$ matches that of the source signal $s(n)$ (up to a scaling).

Let $\boldsymbol{q}(z) \doteq \boldsymbol{a}(z) + \boldsymbol{f}(z)$. From Fig. 2,

$$\boldsymbol{e}(n) = \left[\boldsymbol{I} - \boldsymbol{B}\boldsymbol{q}(z)\boldsymbol{w}^H\right]^{-1} \boldsymbol{B}\left[\boldsymbol{c}(z)s(n) + \boldsymbol{\eta}(n)\right] \tag{12}$$

Denote $\boldsymbol{T}(z) \doteq \left[\boldsymbol{I} - \boldsymbol{B}\boldsymbol{q}(z)\boldsymbol{w}^H\right]^{-1}\boldsymbol{B}$. Then, from (12),

$$\mathbf{S}_{\boldsymbol{ee}} = \boldsymbol{T}\boldsymbol{c}\tilde{\boldsymbol{c}}\tilde{\boldsymbol{T}}\mathsf{S}_{ss} + \boldsymbol{T}\mathbf{S}_{\boldsymbol{\eta\eta}}\tilde{\boldsymbol{T}} \tag{13}$$

where $\tilde{\cdot}$ denotes paraconjugation, i.e., $\tilde{\boldsymbol{A}}(z) \doteq \boldsymbol{A}^H(1/z^*)$. Using the Matrix Inversion Lemma, one finds that

$$\boldsymbol{T}(z) = \boldsymbol{B} + \frac{\boldsymbol{B}\boldsymbol{q}(z)\boldsymbol{w}^H\boldsymbol{B}}{1 - \boldsymbol{w}^H\boldsymbol{B}\boldsymbol{q}(z)}. \tag{14}$$

The output signal is then given by

$$y(n) = \boldsymbol{w}^H\boldsymbol{e}(n) = \boldsymbol{w}^H\boldsymbol{T}(z)\left[\boldsymbol{c}(z)s(n) + \boldsymbol{\eta}(n)\right]. \tag{15}$$

4.2. The high SNR case

A characterization of the stationary points in closed form is not possible for general noise power spectra $\mathbf{S}_{\boldsymbol{\eta\eta}}(z)$ due to the nonlinear nature of the equations involved. The following analysis assumes that the SNR at the relay is high, so that the noise $\boldsymbol{\eta}(n)$ can be neglected, i.e. $\mathbf{S}_{\boldsymbol{\eta\eta}}(z) \approx \mathbf{0}$ in (13). In that case one has $\mathsf{S}_{yy}(z) = [\boldsymbol{w}^H\boldsymbol{T}(z)\boldsymbol{c}(z)][\tilde{\boldsymbol{c}}(z)\tilde{\boldsymbol{T}}(z)\boldsymbol{w}]\mathsf{S}_{ss}(z)$. This fact, together with (11), implies that $\boldsymbol{w}^H\boldsymbol{T}(z)\boldsymbol{c}(z)$ must be an all-pass function, as long as the power spectrum of the source signal satisfies $\mathsf{S}_{ss}(e^{j\omega}) > 0 \; \forall\omega$. Then it follows from

$$\boldsymbol{w}^H\boldsymbol{T}(z)\boldsymbol{c}(z) = \frac{\boldsymbol{w}^H\boldsymbol{B}\boldsymbol{c}(z)}{1 - \boldsymbol{w}^H\boldsymbol{B}\boldsymbol{q}(z)} \tag{16}$$

that, if $\boldsymbol{w}^H\boldsymbol{B}\boldsymbol{c}(z)$ is minimum phase, then $\boldsymbol{w}^H\boldsymbol{T}(z)\boldsymbol{c}(z) = \gamma$ (a constant), and thus $y(n)$ equals $s(n)$ up to a scaling and phase rotation. Note that it may still be possible to have $\boldsymbol{w}^H\boldsymbol{B}\boldsymbol{c}(z)$ minimum phase without requiring all of the individual subchannels (entries of $\boldsymbol{c}(z)$) to be minimum phase[2]. It is seen then that the STFS is simultaneously canceling the feedback path *and* equalizing the source-relay channel.

We then have the following result.

Lemma 1. *Assume $\mathsf{S}_{ss}(e^{j\omega}) > 0 \; \forall\omega$. Then at any stationary point for which $\boldsymbol{w}^H\boldsymbol{B}\boldsymbol{c}(z)$ is minimum phase, then $\boldsymbol{a}(z) = -\boldsymbol{f}(z) - \gamma^{-1}[\boldsymbol{c}(z) - \boldsymbol{c}_0]$.*

Proof. Start with $\boldsymbol{e}(n) = \boldsymbol{T}(z)\boldsymbol{c}(z)s(n)$; then, since the right-hand side of (16) equals γ, from (14) one has

$$\boldsymbol{T}(z)\boldsymbol{c}(z) = \boldsymbol{B}\boldsymbol{c}(z) + \frac{\boldsymbol{B}\boldsymbol{q}(z)\boldsymbol{w}^H\boldsymbol{B}\boldsymbol{c}(z)}{1 - \boldsymbol{w}^H\boldsymbol{B}\boldsymbol{q}(z)} = \boldsymbol{B}[\boldsymbol{c}(z) + \gamma\boldsymbol{q}(z)] \tag{17}$$

so that the power spectrum (13) becomes $\mathbf{S}_{\boldsymbol{ee}} = \mathsf{S}_{ss}\boldsymbol{B}(\boldsymbol{c} + \gamma\boldsymbol{q})(\tilde{\boldsymbol{c}} + \gamma^*\tilde{\boldsymbol{q}})\boldsymbol{B}^H$. Condition (10) reads then as

$$\boldsymbol{B}[\boldsymbol{c}(z) + \gamma\boldsymbol{q}(z)][\tilde{\boldsymbol{c}}(z) + \gamma^*\tilde{\boldsymbol{q}}(z)]\boldsymbol{B}^H\boldsymbol{w} = \boldsymbol{w}. \tag{18}$$

The fact that the right-hand side of (16) equals γ in turn implies that $\boldsymbol{w}^H\boldsymbol{B}[\boldsymbol{c}(z) + \gamma\boldsymbol{q}(z)] = \gamma$, and therefore (18) yields $\gamma^*\boldsymbol{B}[\boldsymbol{c}(z) + \gamma\boldsymbol{q}(z)] = \boldsymbol{w}$. Therefore $\boldsymbol{c}(z) + \gamma\boldsymbol{q}(z)$ must be a zero-degree polynomial, or equivalently $\boldsymbol{a}(z) = -\boldsymbol{f}(z) - \gamma^{-1}[\boldsymbol{c}(z) - \boldsymbol{c}_0]$, since $\boldsymbol{a}$, $\boldsymbol{f}$, $\boldsymbol{q}$ are strictly causal. □

If the conditions in Lemma 1 hold, then the temporal filter of the STFS effectively identifies the feedback path and the strictly causal part of the source-relay channel. Moreover, it then follows from (18) that $\gamma^*\boldsymbol{B}\boldsymbol{c}_0 = \boldsymbol{w}$; writing $\boldsymbol{c}_0 = [c_{01} \; \cdots \; c_{0M}]^T$ this means that

$$\measuredangle(c_{01}b_1w_1^*) = \measuredangle(c_{02}b_2w_2^*) = \cdots = \measuredangle(c_{0M}b_Mw_M^*), \tag{19}$$

i.e., the spatial processor of the STFS achieves phase alignment of the signals at the M branches. Note that this desirable property has been obtained without knowledge about the source-relay channel.

Suppose now that $\boldsymbol{w}^H\boldsymbol{B}\boldsymbol{c}(z)$ is not minimum phase at the stationary point. One still has $\boldsymbol{w}^H\boldsymbol{T}(z)\boldsymbol{c}(z) = v(z)$, where $v(z)$ is an allpass function: $v(z)\tilde{v}(z) = |\gamma|^2$. Following analogous steps to those in the proof of Lemma 1, it can be shown that $\boldsymbol{e}(n) = \frac{1}{|\gamma|^2}\boldsymbol{w}v(z)s(n)$, and consequently the signals $w_i^*e_i(n) = \frac{|w_i|^2}{|\gamma|^2}v(z)s(n)$ are again phase aligned. The residual distortion in the relay output $y(n) = v(z)s(n)$ when the allpass function $v(z)$ is not a constant is due to the fact that only second-order statistical information about the desired signal $s(n)$ is being exploited.

5. SIMULATION RESULTS

We present an illustrative scenario similar to that in [10] to show the behaviour of the algorithm. The source signal is a 16-QAM square-root raised cosine filtered signal with roll-off $\alpha = 1$, so that the corresponding normalized autocorrelation (6) is $r_0 = 1$, $r_1 = 0.5$, $r_k = 0$, $k > 1$. The relay demodulates the received signals to baseband and then samples them at twice the baud rate. The number of receive antennas is $M = 3$, with separation $d = \lambda/2$. It is assumed that $g_0(z) = 1$, whereas $\boldsymbol{G}(z) = z^{-\delta}\boldsymbol{I}$, with $\delta = 6$ modeling the delay due to the analog filters in the receive front-end.

[2]Certainly, there are cases for which this is not possible. For example, if $\boldsymbol{c}(z) = (1 - z_0z^{-1})\boldsymbol{c}'(z)$ with $|z_0| > 1$.

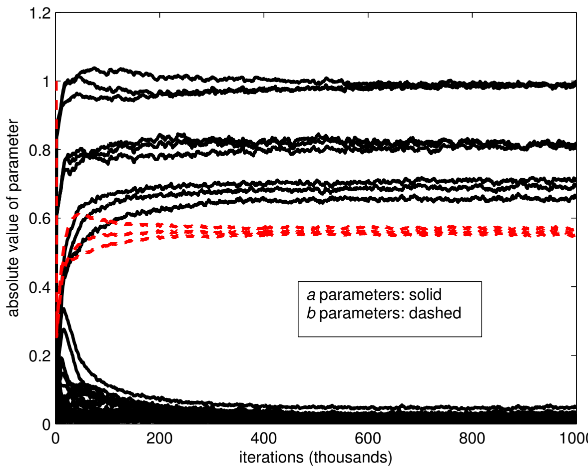

Fig. 3. Evolution of the adaptive parameters. SNR $= 20$ dB.

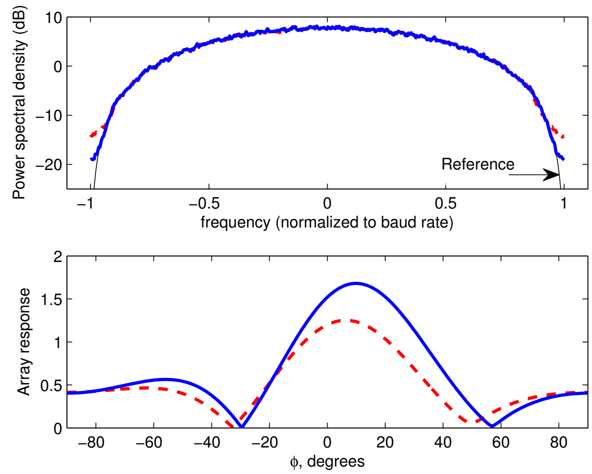

Fig. 5. Top: Power spectrum of the STFS output signal. Bottom: Array response. SNR $= 20$ dB (solid), 5 dB (dashed).

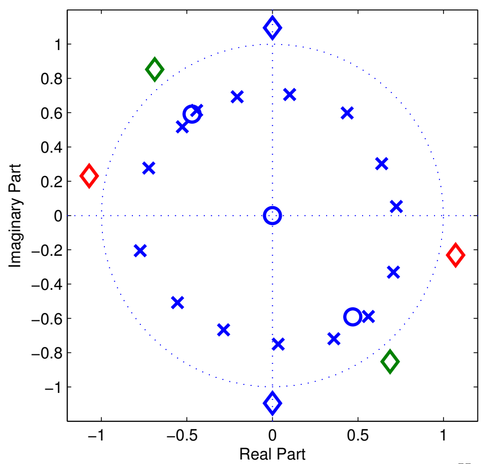

Fig. 4. Zeros of the source-relay subchannels ($\diamond$), of $\boldsymbol{w}^H\boldsymbol{B}\boldsymbol{c}(z)$ ($\circ$) and of $1-\boldsymbol{w}^H\boldsymbol{B}\boldsymbol{q}(z)$ ($\times$). SNR $= 20$ dB.

Both the source-relay channel $\boldsymbol{d}(\omega)$ and the self-interference channel $\boldsymbol{p}(\omega)$ consist of two paths each, with parameters

$$\beta_1^s = 1, \quad \Delta_1^{(s)} = 0, \quad \phi_1^{(s)} = 10^\circ, \tag{20}$$

$$\beta_2^s = 1.2, \quad \Delta_2^{(s)} = 2T_s, \quad \phi_2^{(s)} = -15^\circ, \tag{21}$$

$$\beta_1^r = 1, \quad \Delta_1^{(r)} = T_s, \quad \phi_1^{(r)} = 14^\circ, \tag{22}$$

$$\beta_2^r = 0.8, \quad \Delta_2^{(r)} = 2T_s, \quad \phi_2^{(r)} = 6^\circ. \tag{23}$$

Spatially- and temporally-white noise (i.e. $\mathsf{S}_{\boldsymbol{\eta}\boldsymbol{\eta}}(z) = \sigma_\eta^2 \boldsymbol{I}_M$) is added to the received signals. The SNR is defined as SNR $= \frac{1}{M\sigma_\eta^2}\sum_i \sum_j r_{i-j}\boldsymbol{c}_i^H \boldsymbol{c}_j$.

The adaptive filter has order $L_a = 15$, and we fix $\boldsymbol{w} = \boldsymbol{1}$. The stepsize values are $\mu_a = 5 \times 10^{-5}$ and $\mu_b = 10^{-4}$.

The trajectories of the adaptive parameters in this scenario, with SNR $= 20$ dB, are shown in Fig. 3. The initial values were $\boldsymbol{B} = \boldsymbol{I}_M$ and $\boldsymbol{a}(z) = \boldsymbol{0}$. For this choice of stepsizes, convergence is quite smooth and takes less than 10^6 iterations. Fig. 4 shows the poles and zeros of the overall transfer function $\boldsymbol{w}^H\boldsymbol{T}(z)\boldsymbol{c}(z)$ from (16) attained at the stationary point. It is observed that the STFS has converged to a setting at which the numerator $\boldsymbol{w}^H\boldsymbol{B}\boldsymbol{c}(z)$ is minimum phase (even though neither of the individual subchannels $\boldsymbol{c}(z)$ has this property, as seen also in Fig. 4), and accordingly, the denominator places some of its roots so as to have pole-zero cancellations. The remaining poles are approximately equispaced on a circle and have little impact on the overall transfer function; they appear due to the tail coefficients of $\boldsymbol{a}(z)$, which take small but nonzero values (see also Fig. 3). The output power spectrum $\mathsf{S}_{yy}(e^{j\omega})$ attained after convergence for SNR $=$ 20 and 5 dB, together with the reference spectrum, are shown in Fig. 5, illustrating the restoral property of the algorithm. The same figure also depicts the array response $|\boldsymbol{w}^H\boldsymbol{B}\boldsymbol{v}(\phi)|$ for these two SNR values. As expected, since $\boldsymbol{w}^H\boldsymbol{B}\boldsymbol{c}(z)$ is minimum phase at convergence, the adaptive array locks on to the direction of the first arrival from the source transmitter (10° in this example). Thus, the proposed adaptive STFS has effectively canceled the relay self-interference, and simultaneously it provides equalization for the source-relay channel. It must be noted that, in steady-state, the signal-to-self-interference ratio at the relay input is approximately -4.5 dB. Under these conditions, an STFS based on spatial processing alone and without knowledge of the AoA of the sourcce signal would have a hard time in order to avoid locking to the self-interfering signal.

6. CONCLUDING REMARKS

A new blind adaptive scheme for spatio-temporal suppression of self-interference in full-duplex relays has been presented. The method is effective and is capable of partially mitigating multipath propagation in the source-to-relay channel. The only information required is knowledge of the power spectrum of the source signal, since the basis of the algorithm is the restoration of said power spectrum at the relay output. In particular, the new scheme does not require knowledge of the AoA of the source signal, in contrast with previous approaches. This is achieved at the cost of having M adaptive filters in parallel, whereas just one of these suffices when AoA information is available. Future work will focus on developing AoA-blind schemes with reduced complexity.

7. REFERENCES

[1] D. W. Bliss, P. A. Parker, and A. R. Margetts, "Simultaneous transmission and reception for improved wireless network performance," in *Proc. IEEE 14th Workshop Stat. Signal Process.*, Aug. 2007.

[2] M. Duarte, C. Dick, and A. Sabharwal, "Experiment-driven characterization of full-duplex wireless systems," *IEEE Trans. Wireless Commun.*, vol. 11, no. 12, pp. 4296 – 4307, dec 2012.

[3] K. Haneda, E. Kahra, S. Wyne, C. Icheln, and P. Vainikainen, "Measurement of loop-back interference channels for outdoor-to-indoor full-duplex radio relays," in *Proc. 4th European Conference on Antennas and Propagation*, Apr. 2010.

[4] P. Larsson and M. Prytz, "MIMO on-frequency repeater with self-interference cancellation and mitigation," in *Proc. IEEE 69th Veh. Technol. Conf.*, Apr. 2009.

[5] P. Lioliou, M. Viberg, M. Coldrey, and F. Athley, "Self-interference suppression in full-duplex MIMO relays," in *Proc. Asilomar Conf. Signals, Syst., Comput.*, 2010.

[6] T. Riihonen, S. Werner, and R. Wichman, "Mitigation of loop-back self-interference in full-duplex MIMO relays," *IEEE Trans. Signal Process.*, vol. 59, no. 12, pp. 5983 –5993, Dec. 2011.

[7] J.-H. Lee and O.-S. Shin, "Full-duplex relay based on block diagonalisation in multiple-input multiple-output relay systems," *IET Commun.*, vol. 4, no. 15, pp. 1817 –1826, 2010.

[8] R. López-Valcarce, E. Antonio-Rodríguez, C. Mosquera, and F. Pérez-González, "An adaptive feedback canceller for full-duplex relays based on spectrum shaping," *IEEE J. Sel. Areas Commun.*, vol. 30, no. 8, pp. 1566–1577, 2012.

[9] S. Berger et al., "Recent advances in amplify-and-forward two-hop relaying," *IEEE Commun. Mag.*, vol. 47, no. 7, pp. 50–56, 2009.

[10] E. Antonio-Rodríguez and R. López-Valcarce, "Adaptive self-interference suppression for full-duplex relays with multiple receive antennas," in *Proc. 13th IEEE Int. Workshop Signal Process. Adv. Wireless Commun.*, 2012.

[11] A. M. Sayeed, "Deconstructing multiantenna fading channels," *IEEE Trans. Signal Process.*, vol. 50, no. 10, pp. 2563–2579, 2002.

[12] D. G. Manolakis, V. K. Ingle, and S. M. Kogon, *Statistical and adaptive signal processing*, McGraw-Hill, 2000.